



# Experimental validation of a dynamic model of energy ships

Baptiste Elie, Olivier Kermorgant, Aurelien Babarit, Vincent Fremont,  
Juin-Gauthier Giovanni

## ► To cite this version:

Baptiste Elie, Olivier Kermorgant, Aurelien Babarit, Vincent Fremont, Juin-Gauthier Giovanni. Experimental validation of a dynamic model of energy ships. 25e Congrès Français de Mécanique, Nantes, Aug 2022, Nantes, France. hal-04280190

**HAL Id: hal-04280190**

**<https://hal.science/hal-04280190v1>**

Submitted on 13 Nov 2023

**HAL** is a multi-disciplinary open access archive for the deposit and dissemination of scientific research documents, whether they are published or not. The documents may come from teaching and research institutions in France or abroad, or from public or private research centers.

L'archive ouverte pluridisciplinaire **HAL**, est destinée au dépôt et à la diffusion de documents scientifiques de niveau recherche, publiés ou non, émanant des établissements d'enseignement et de recherche français ou étrangers, des laboratoires publics ou privés.

# Experimental validation of a dynamic model of energy ships

**G. JUIN-GAUTHIER<sup>a</sup>, B. ELIE<sup>b</sup>, O. KERMORGANT<sup>c</sup>, A. BABARIT<sup>d</sup>, V. FREMONT<sup>e</sup>**

a. Nantes Université, École Centrale Nantes, LS2N, juin-gauthier.giovanni@ls2n.fr

b. Farwind Energy, baptiste.elie@farwind-energy.com

c. Nantes Université, École Centrale Nantes, LS2N, olivier.kermorgant@ec-nantes.fr

d. Farwind Energy, aurelien.babarit@farwind-energy.com

e. Nantes Université, École Centrale Nantes, LS2N, vincent.fremont@ec-nantes.fr

## Résumé :

*Récupérer l'énergie du vent loin en mer avec des éoliennes classiques (posées ou flottantes) serait aujourd'hui compliqué et coûteux [1]. Le voilier à énergie est une solution à ce problème. Il s'agit d'un navire propulsé par des voiles, sous lequel se trouvent des hydrogénérateurs. Ces hydrogénérateurs produisent de l'électricité à partir de l'énergie cinétique disponible dans le courant relatif créé par le navire. Un prototype a été conçu et testé sur le lac de Vioreau par l'École Centrale de Nantes et Farwind Energy, afin de prouver le concept [8]. Un modèle dynamique du prototype a été développé pour tester différentes architectures de contrôleurs et pour étudier le comportement du navire. Les prédictions du modèle ont été comparées aux données expérimentales pour validation. Cette étude a montré que le modèle fournissait avec précision la vitesse d'avance du bateau, mais prévoyait moins bien l'angle de barre nécessaire pour maintenir le bateau à cap constant.*

## Abstract :

*Harvesting far offshore wind energy is for now challenging and costly with traditional offshore wind turbines [1]. The energy ship is a concept to address this issue. It consists in a vessel propelled using sails, under which hydro turbines are attached. These hydro turbines produce electricity from the kinetic energy available in the relative current created by the sailing boat. A remotely operated prototype of energy ship has been created and tested on the Vioreau lake (France) by École Centrale de Nantes and the company Farwind Energy in order to prove the concept of energy ship [8]. A dynamic model of the prototype has been developed to test different controller architectures and to investigate the behaviour of the prototype. The predictions given by the dynamic model have been compared with the experimental results for validation. The comparisons show that the model is well designed to predict the boat speed at equilibrium, while being less effective in the prediction of the rudder angle required to maintain the ship in a straight line.*

**Mots clefs : Energy ship, Flettner rotor, Wind energy, Water turbine, Dynamic model**

# 1 Introduction

The energy ship is a new concept for offshore wind energy capture. It consists in a vessel propelled using sails, under which water turbines are installed. The kinematic energy of the ship is converted by the turbines into electricity. The generated energy is stored on board, in batteries or is directly used to produce fuel onboard (hydrogen, ammonia, methanol, etc... [2]). The main advantage of this technology is that it allows to harvest energy in the high seas, where conventional wind turbines are challenging due to the grid connection costs, installation costs and operation costs increasing with distance to shore.

The concept of the energy ship was patented in 1982 [3]. However, it did not receive much attention until the end of the first decade of the 2000s. Regarding academic works, the energy ship has also been the focus of only few studies, most of which are limited to theoretical and numerical studies [4]- [5]. The first experimental study was carried out in 2019 on the Erdre river in France by École Centrale de Nantes [6]. That study allowed on the one hand to experimentally investigate the effect of the water turbine drag on energy production and on the other hand to verify that significant quantities of energy can be produced by the energy ship. A prototype was specially developed for that purpose using a Hobie Cat Tiger catamaran as a starting point. A second version of the prototype has been developed and tested by École Centrale de Nantes and Farwind Energy [8] (figure 1). The objectives of this second experimental campaign were twofold. First, it was to achieve an experimental validation of an energy ship propelled by a Flettner rotor, and remotely controlled. Second, it was to generate experimental data suitable for validation of numerical models which can be used to estimate the performance of energy ships at full-scale.

The energy ship is a concept which aims at producing clean energy from offshore wind. Therefore, it is

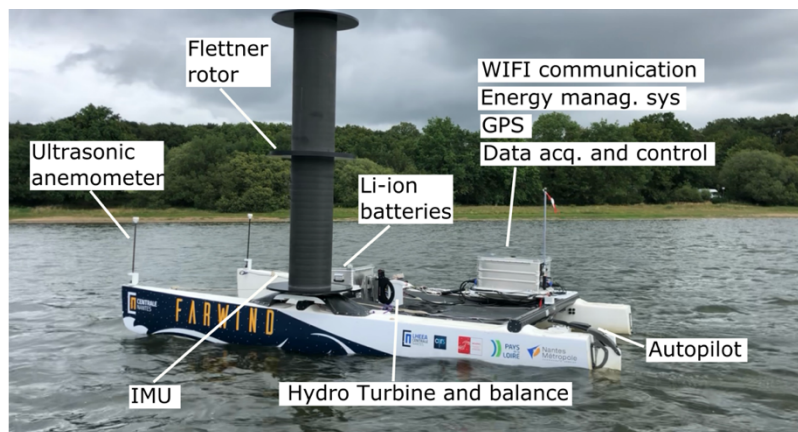


FIGURE 1 – Second prototype of the energy ship

necessary to optimise the control of the active components of the ship (Flettner rotor rotational velocity, water turbine rotational velocity and rudder angle), to extract maximum energy in given conditions. A dynamic numerical model is currently under development for this purpose. The objectives of this model are twofold. First, it will allow to test different controller architectures, especially model based control laws. Second, it will make it possible to investigate the behaviour of the energy ships depending on their design and to validate navigation strategies for its different sailing modes. Validation of the model is achieved by comparing numerical simulations to experimental data.

This paper is organised as follows : first the model of the energy ship developed is described in section 2. Then the experimental procedure and comparison to the model results is presented in section 3.

## 2 Dynamic model of the energy ship

In this section the dynamic model of the energy ship is presented. It consists in a dynamic and kinematic equation and in the forces models used to represent the forces on the ship.

### 2.1 Dynamic equation and kinematic equation

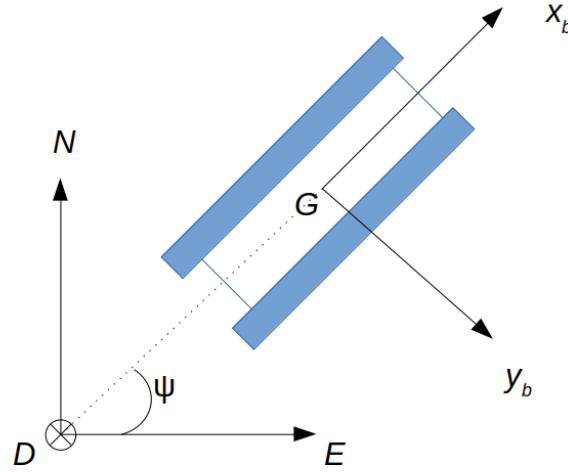


FIGURE 2 – Coordinates systems

Several simplifications are made regarding the ship's motion. Only the three horizontal degrees of freedom are considered (sway, surge and yaw). The motion of the ship is represented in two frames of reference. The North-East-Down (NED) reference frame, which can be assumed inertial in the case of "flat Earth navigation" [9], is defined as the plane tangent to the surface of the Earth at the localization of the ship. The body fixed reference  $(G, x_b, y_b)$  frame is a moving frame fixed to the ship. The frames are shown in the figure 2. The position of the ship in the NED reference frame is denoted  $\eta$ . The velocities of the ship are denoted in the body frame as the vector  $\nu$ .

$$\eta = \begin{pmatrix} N \\ E \\ \psi \end{pmatrix} \quad \nu = \begin{pmatrix} u \\ v \\ r \end{pmatrix}$$

The kinematic and the dynamic equations are written as vectorial equations. The kinematic equation can be written :

$$\dot{\eta} = R(\psi)\nu \quad (1)$$

with  $R(\psi) = \begin{pmatrix} \cos \psi & -\sin \psi & 0 \\ \sin \psi & \cos \psi & 0 \\ 0 & 0 & 1 \end{pmatrix}$ , the rotational matrix between the body frame and the NED frame.

The dynamic equation can be written :

$$M\dot{\nu} + C(\nu)\nu = \tau \quad (2)$$

with  $M$  being the mass matrix of the boat, which includes the rigid-body mass matrix and the added-mass matrix,  $C$  the Coriolis matrix, which includes the rigid-body Coriolis matrix and the added-mass Coriolis matrix and  $\tau$ , the forces acting on the ship.

$$M = M_{RB} + M_A = \begin{pmatrix} m & 0 & 0 \\ 0 & m & 0 \\ 0 & 0 & I_z \end{pmatrix} + \begin{pmatrix} -X_{\dot{u}} & 0 & 0 \\ 0 & -Y_{\dot{v}} & 0 \\ 0 & 0 & -N_{\dot{r}} \end{pmatrix} \text{ at the center of gravity of the ship [9].}$$

$$C(\nu) = C_{RB}(\nu) + C_A(\nu) = \begin{pmatrix} 0 & 0 & -mv \\ 0 & 0 & mu \\ mv & -mu & 0 \end{pmatrix} + \begin{pmatrix} 0 & 0 & Y_{\dot{v}}v \\ 0 & 0 & -X_{\dot{u}}u \\ -Y_{\dot{v}}v & X_{\dot{u}}u & 0 \end{pmatrix} \text{ at the center of gravity of the ship [9]-[10].}$$

With  $m$  being the mass of the ship,  $I_z$  the yaw moment of the ship and  $X_{\dot{u}}$ ,  $Y_{\dot{v}}$  and  $N_{\dot{r}}$  being the added inertia on the ship, estimated with the approximations and simplifications of Hadi Saoud [10].

## 2.2 Forces models

Components of the ship that generate a force acting on the ship are the Flettner rotors, the hulls, the appendages, the rudders and the water turbine. These forces are modelled as follows :

- The force of the rotor is divided in two different forces. The drag force ( $D$ ), which is oriented along the wind flow direction and the lift force ( $L$ ), which is perpendicular to the wind flow direction, as shown in figure 3. The lift ( $C_l$ ) and drag ( $C_d$ ) coefficients are defined so that :

$$D = \frac{1}{2} C_d \rho_{air} V^2 A_R$$

$$L = \frac{1}{2} C_l \rho_{air} V^2 A_R$$

with  $A_R$  the projected surface of the rotor in the flow direction,  $V$  the apparent wind speed and  $\rho_{air}$  the density of air.

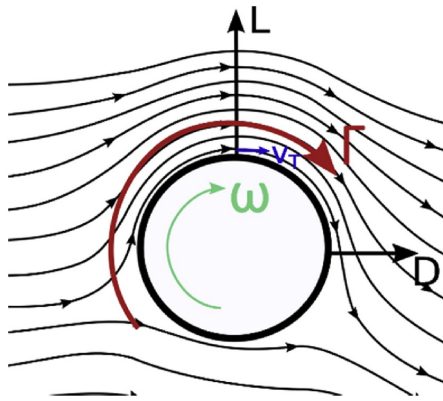


FIGURE 3 – Schematic of forces and wind flow around the rotor [11]

Models for the lift and drag coefficients of Flettner rotors have been proposed in [12] and [11]. The drag and the lift coefficients of the rotor depends on the spin ratio ( $SR$ ) of the rotor, which is the ratio between the apparent wind speed and the tangential speed of the rotor's surface.

$$SR = \frac{\omega R_R}{V},$$

with  $\omega$  being the rotational speed of the rotor,  $R_R$  the radius of the rotor [11].

In [11] a polynomial approximation of the coefficients has been proposed whereas a table of coefficients is proposed in [12]. For the model of the energy ship, the model of [12] has been used,

since the Reynolds number matches better with that of the experiments.

- The hull's force is modeled by two different forces. The first is the water resistance. It is proportional to the square of the boat speed and depends on the shape and dimensions of the hull [16]. The second force is related to the lift effect of the hull [11]. It depends on the drift angle of the ship.
- The rudder and the appendages are considered to be NACA 0009 profiles. The force of such profiles can be separated between a drag force in the direction of the flow and a lift force, perpendicular to the flow. [14] proposes a table of the lift and drag coefficients for NACA 0009 profiles, depending on the angle of attack of the flow relative to the neutral line of the profile.
- The effect of the water turbine is modelled using a table of the drag force depending on the boat speed and on the control of the water turbine. This table is based on towing tank experiments that have been conducted in order to characterise the turbine. We refer the reader to [6] for a more detailed description of these experiments.

## 2.3 Solving the dynamic and kinematic equations

Equations 1 and 2 are solved using a Runge-Kutta 4 integration scheme with a fixed time step. The integration scheme is defined as follows, with  $q$  being the state-vector and  $h$  being the time step :

- $q_0$ , the initial state vector is provided by the user of the model.
- Knowing  $q_n$  it is possible to calculate  $k_1$  such as  $k_1 = f(t_n, q_n)$  with  $f$  being the motion equation ( $\dot{q} = f(t, q)$ , in our case it is the concatenation of equations 1 and 2).
- The  $k_2$  term is defined such as  $k_2 = f(t_n + h/2, q_n + \frac{h}{2}k_1)$ .
- The  $k_3$  term is defined such as  $k_3 = f(t_n + h/2, q_n + \frac{h}{2}k_2)$ .
- The  $k_4$  term is defined such as  $k_4 = f(t_n + h, q_n + hk_3)$ .
- The state vector at the next time step is then defined as  $q_{n+1} = q_n + \frac{h}{6}(k_1 + 2k_2 + 2k_3 + k_4)$ .

This method has the advantage of being stable and precise [15].

## 3 Comparison between experimental and numerical results

### 3.1 Experimental campaign

A prototype of energy ship was developed using a Hobie Cat Tiger catamaran as a starting point (figure 1). Its rig (mast plus a mainsail and a jib) has been replaced by a Flettner rotor mounted on the port side float of the hull. The energy production is achieved using a water turbine installed between the two hulls. The ship only has one dagger board on the port hull and one rudder at the end of the port float. Experiments were carried out in late June 2021 on the Vioreau lake (France), under light wind conditions (3 to 11 knots). The experimental method consisted in a series of roundtrips on beam reach as described in figure 4. This wind direction was chosen because it corresponds to the point of sail for which the performance of the energy ship is maximum. On each round trip, the control settings (Flettner rotor's rotational velocity and water turbine output voltage) were changed to study their effect on the energy production and on the ship's behavior. Experimental data was first processed in order to remove cases for which the true wind speed (TWS) was too low or for which there was sudden changes in the

true wind angle (TWA). This was necessary to get data corresponding to steady conditions, allowing the validation of the forces models, by eliminating the dynamic component of equation (2). Only the beam reach and constant SR time ranges have been retained (i.e. : the trips for which standard deviation of the TWA and TWS is small (inferior to  $5^\circ$  on TWA and inferior to 1 m/s for TWS as can be seen in table 1)). The signals were then averaged over each of these time intervals. Each case lasted for about 30 seconds. Standard deviations around the mean value for each case were also calculated in order to keep track of the data quality. These data are presented in table 1.

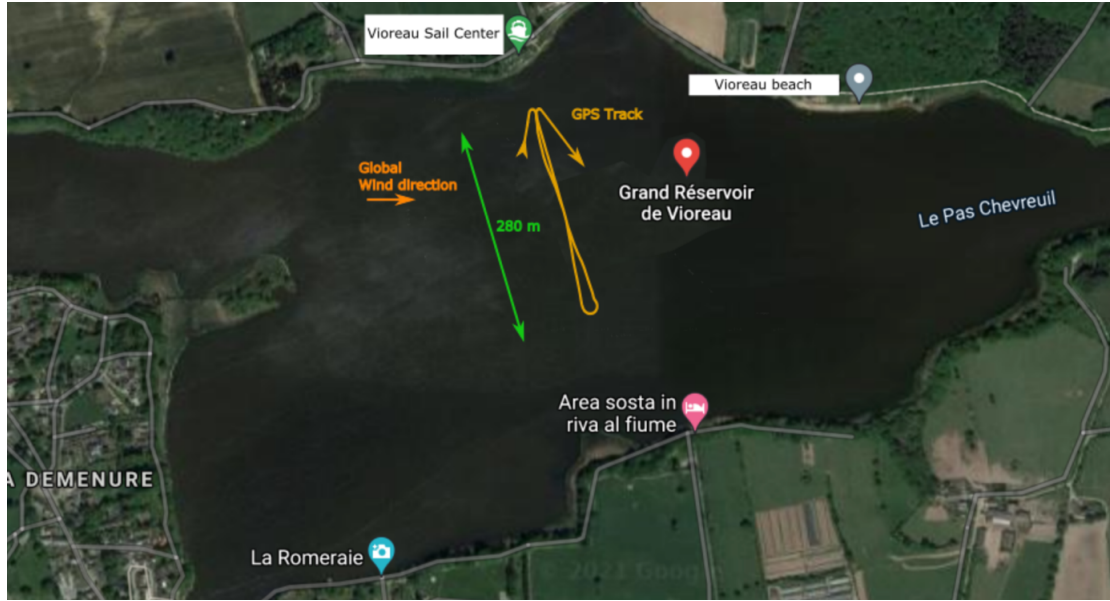


FIGURE 4 – Example of GPS track during the experimentation

| Case | Mean TWA ( $^\circ$ ) | Std ( $^\circ$ ) | Mean TWS (m/s) | Std (m/s) | $\omega$ Flettner rotor (rpm) | SR   | Water Turbine Tension (V) | Boat speed (m/s) | Std (m/s) | Rudder angle ( $^\circ$ ) |
|------|-----------------------|------------------|----------------|-----------|-------------------------------|------|---------------------------|------------------|-----------|---------------------------|
| 11   | -93,8                 | 3,27             | 4,71           | 0,55      | 700                           | 3,30 | 42,2                      | 1,97             | 0,04      | -4.97                     |
| 13   | 98,3                  | 4,77             | 4,85           | 0,85      | -700                          | 3,33 | 41,3                      | 1,85             | 0,12      | 1.52                      |
| 16   | 83,3                  | 2,60             | 4,49           | 0,60      | -686                          | 3,31 | 30,9                      | 1,67             | 0,04      | 5.28                      |
| 17   | -100,0                | 2,74             | 4,11           | 0,51      | 700                           | 4,03 | 32,5                      | 1,79             | 0,07      | -5.91                     |
| 20   | -96,0                 | 4,25             | 3,79           | 0,52      | 489                           | 2,84 | 26,6                      | 1,52             | 0,05      | -5.10                     |
| 22   | 90,0                  | 3,22             | 4,09           | 0,58      | -698                          | 3,67 | 22,1                      | 1,62             | 0,07      | 4.85                      |
| 23   | -91,8                 | 2,95             | 4,36           | 0,79      | 700                           | 3,58 | 22,4                      | 1,75             | 0,05      | -5.94                     |
| 27   | 90,7                  | 3,21             | 5,04           | 0,49      | -692                          | 3,14 | 12,2                      | 1,72             | 0,14      | 4.12                      |

TABLE 1 – Curated data

## 3.2 Methodology

Table 1 shows the experimental results which have been used for the validation of the dynamic model presented in section 2. To do so, some values are used as inputs to the model in order to replicate the experimental test cases numerically, while others are used for comparisons with the numerical model outputs to assess the ability of the model to predict the behaviour of the experimental platform.

— Inputs : Wind (angle and speed), Flettner rotor rotational speed, water turbine control.

— Outputs : Boat speed and rudder angle required to maintain the boat in a straight line.

Comparing the boat speeds allows to validate the linear forces model of the ship, while the rudder angles comparison validates the torques model of the different components of the ship.

The wind standard deviation observed during the experiments is taken into account for each cases using a randomly generated set of 20 values (magnitude and angle), normally distributed around the mean value given in table 1. Hence, 400 operating points are tested for each experimental case.

The initial conditions of the model in each simulation are the same. The ship is supposed to be initially at rest (no speed), then the simulation lasts until the ship reaches its equilibrium. Finally, the last ship's state obtained during the simulation is compared with the experimental results. This comparison is presented in section 3.3.

### 3.3 Results

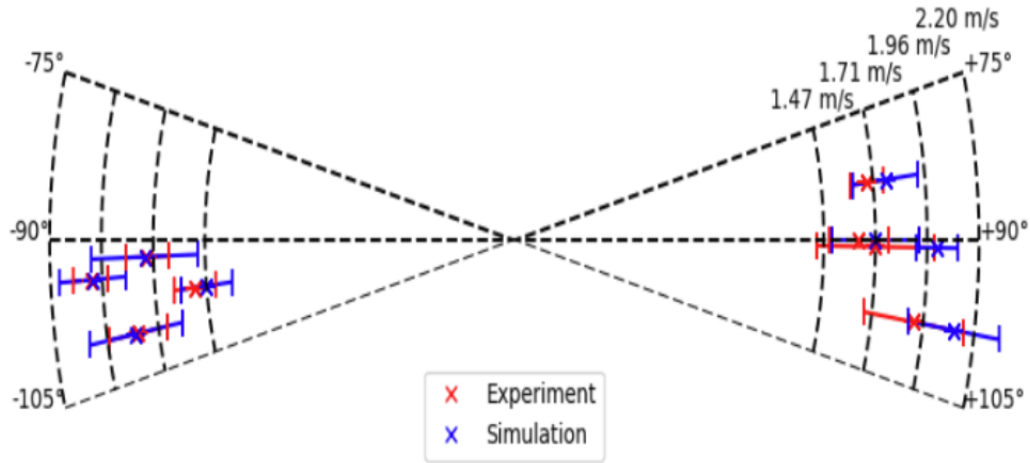


FIGURE 5 – Comparison of the measured boat speeds (in red) and the predicted boat speeds (in blue), standard deviation represented as the error bars.

Figure 5 shows a comparison between the experimental and model boat speeds as a function of wind direction. The standard deviations of both the measurements and simulations are represented as error bars on the graph.



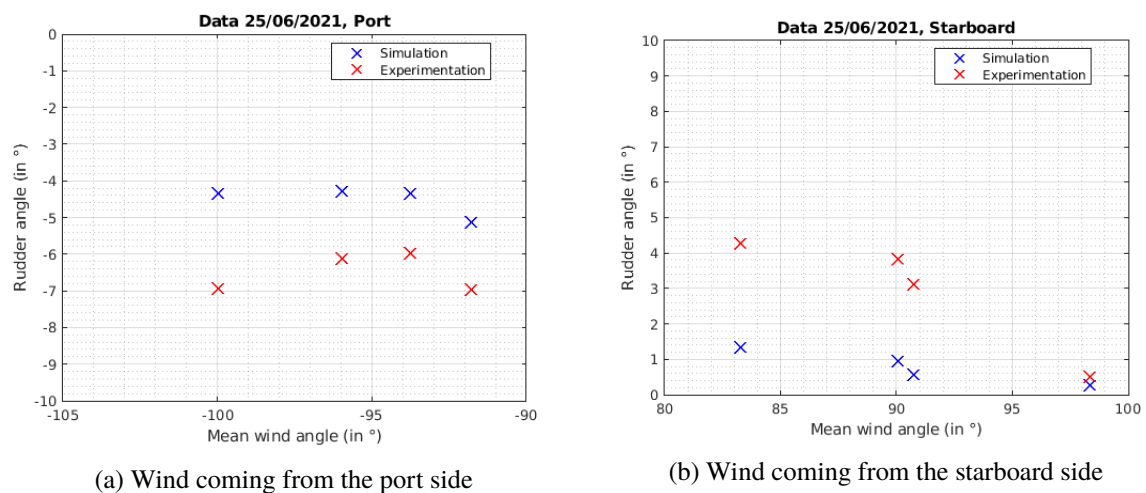


FIGURE 6 – Rudder angles (model and experimentation)

Figures 6a and 6b present the mean angle of the rudder to maintain the ship in a straight line as a function of wind direction.

| Case | Wind Angle (in °) | Boat speed (model) (in m/s) | Boat speed (experimental) (in m/s) | Boat speed relative error (in %) |
|------|-------------------|-----------------------------|------------------------------------|----------------------------------|
| 17   | -100.0            | 1.82                        | 1.81                               | 0.4                              |
| 20   | -96.00            | 1.47                        | 1.52                               | -3.6                             |
| 11   | -93.80            | 2.00                        | 2.01                               | -0.5                             |
| 23   | -91.80            | 1.75                        | 1.74                               | 0.6                              |
| 16   | 83.30             | 1.77                        | 1.68                               | 5.4                              |
| 22   | 90.00             | 1.71                        | 1.63                               | 4.9                              |
| 27   | 90.70             | 2.00                        | 1.71                               | 17.0                             |
| 13   | 98.30             | 2.10                        | 1.91                               | 9.9                              |

TABLE 2 – Comparison between model and experimental boat speeds

| Case | Wind Angle (in °) | Rudder angle (model) (in °) | Rudder angle (experimental) (in °) | Rudder angle relative error (in %) |
|------|-------------------|-----------------------------|------------------------------------|------------------------------------|
| 17   | -100.0            | -4.33                       | -5.91                              | -26.8                              |
| 20   | -96.00            | -4.28                       | -5.10                              | -16.1                              |
| 11   | -93.80            | -4.32                       | -4.97                              | -13.1                              |
| 23   | -91.80            | -5.13                       | -5.94                              | -13.7                              |
| 16   | 83.30             | 1.36                        | 5.28                               | -74.2                              |
| 22   | 90.00             | 0.95                        | 4.85                               | -80.4                              |
| 27   | 90.70             | 0.58                        | 4.12                               | -86.0                              |
| 13   | 98.30             | 0.28                        | 1.52                               | -81.7                              |

TABLE 3 – Comparison between model and experimental rudder angles

The tables 2 and 3 show the error on the speed and the rudder angle between the model and the experi-

ments normalized by the experimental value and expressed in percent.

### 3.4 Discussion

The two metrics used to assess the ability of the numerical model to predict the behaviour of an energy ship are the boat speed, which can validate the linear forces models and the rudder angle, which can validate the torques models. As it can be seen in both figure 5 and table 2, the speed error is relatively small in most cases. In fact only one case presents a relative speed error in excess of 10%. Re-analysis of the experimental data has shown that the ship was not at equilibrium, it was still accelerating. This means that the mean experimental speed was smaller than the actual equilibrium speed. This observation is consistent with the result of the model, which predicts a faster equilibrium speed than the mean experimental speed.

For most cases, the rudder angle error is far more important than the boat speed error. Actually, the numerical model always significantly underpredicts the rudder angle measured experimentally. The origin of this error has not yet been identified. It may be related to an overestimation of the rudder torque, or appendix torque, or/and hull torque around the vertical axis or/and an underestimation of the rotor torque around the vertical axis, at the rotation point. These errors might come from the dimensions and placements of the elements (especially the appendix and rudder). Moreover, the Flettner rotor's motor torque is not taken into account in the model yet. This shortcoming might contribute to this discrepancy between the experimental and the numerical results.

The results on speed are good, as the relative errors are less than 10%. But one can ask if the error on the rudder angle could lead to an error on the speed. Since the force of the rudder is small compared to that of the other elements of the ship, rudder angle errors only have a small impact on the boat speed. So the good results in speed are still valid despite the rudder angle errors. These good results in speed indicate that the model for the linear forces of the elements are representative of the reality.

## 4 Conclusion

The good agreement between the numerical and experimental results for the boat speed seems to validate the model of the linear forces used to define the theoretical model of the ship. But the less satisfying results concerning the rudder angle tends to point out an error of modelling on the boat's torque.

A limitation of this study is that the results are only for steady states. As it can be seen on case test 27, this study was not able to represent dynamic motions of the ship. Only equilibrium positions of the ship have been studied and compared. For this reason, the dynamic terms of equation (2) ( $M$  and  $C$  matrices) cannot be identified and are only estimated using models presented by [10]-[9], for now. There are solutions to identify those parameters using experimental data. Knowing that the force models are representative of the reality, one can use these models and the dynamic equation to identify the dynamic parameters [13].

For these reasons, a new experimental campaign will be necessary, for both exploring the operating points which have not really been explored yet. Especially reaching different points of sail (closed-haul and broad reach) to study the behaviour of the ship in these conditions. This new campaign will also be necessary to generate experimental data adapted for identification process (for instance applying 3211-like inputs to the rudder [17]), allowing the estimation of the dynamic parameters of the system.

## Références

- [1] Offshore wind programme board, Transmission costs for offshore wind, Final report, April 2016
- [2] A. Babarit, J-C Gilloteaux, E. Body, J-F Hétet, Energy and economic performance of the FARWIND energy system for sustainable fuel production from the far-offshore wind energy resource. Proc. Of the 14th International Conference on Ecological Vehicles and Renewable Energies (EVER), Monaco, 2019.
- [3] RE Salomon, Process of converting wind energy to elemental hydrogen and apparatus therefore. U.S. Patent 4335093A, 1982.
- [4] J. Kim, C. Park, Wind power generation with a parawing on ships, a proposal. Energy 2010, Vol.35, pp.1425–1432
- [5] R. Abd-Jamil, A. Chaigneau, J-C Gilloteaux, P. Lelong, A. Babarit, Comparison of the capacity factor of stationary wind turbines and weather-routed energy ships in the far-offshore. Journal of Physics : conference series, 2019, Vol. 1356
- [6] A. Babarit, N. Abdul Ghani, E. Brouillette, S. Delvoye, M. Weber, A. Merrien, M. Michou, J-C Gilloteaux, Experimental validation of the energy ship concept for far-offshore wind energy conversion. Ocean Engineering, 2021, Vol. 239
- [7] A. Babarit, G. Clodic, S. Delvoye, J-C. Gilloteaux, Exploitation of the far-offshore wind energy resource by fleets of energy ships. Part A. Energy ship design and performance. Energy Science, 2020, Vol. 5
- [8] B. Elie, B. Bognet, T. Boileau, M. Weber, J-C. Gilloteaux, A. Babarit Experimental proof-of-concept of an energy ship propelled by a Flettner rotor 2022, TORQUE conference
- [9] T. I. Fossen, Handbook of Marine Craft Hydrodynamics and Motion Control, John Wiley & Sons Ltd, 2011, First edition, ISBN : 978-1-119-99149-6
- [10] H. Saoud, Modélisation et commande de voiliers autonomes. 2016, Thèse, Université Pierre et Marie Curie - Paris VI,
- [11] F. Tillig, J. W. Rinsberg, Design, operation and analysis of wind-assisted cargo ships, Ocean Engineering, 2020, Vol 211
- [12] B. Charrier, Etude théorique et expérimental de l'effet "Magnus" destiné à la propulsion des navires, Thèse, 1979, Université de Paris VI
- [13] G. Peeters, R. Boonen, M. Vanierschot, M. DeFilippo, P. Robinette, P. Slaets, Asymmetric Steering Hydrodynamics Identification of a Differential Drive Unmanned Surface Vessel, 2018, IFAC-PapersOnLine
- [14] R. E. Sheldahl, P. C. Klimas, Aerodynamic characteristics of seven symmetrical airfoil sections through 180-degree angle of attack for use in aerodynamic analysis of vertical axis wind turbines, 1981.
- [15] J.C. Butcher, A history of Runge-Kutta methods, Applied Numerical Mathematics, 1996, Vol. 20
- [16] H. Zakerdoost, H. Ghassemi, M. Ghiasi, An evolutionary optimization technique applied to resistance reduction of the ship hull form, Journal of Naval Architecture and Marine Engineering, 2013

- [17] E. Plaetschke, J. A. Mulder, J. H. Breeman, Flight test results of five input signals for aircraft parameter identification, IFAC Proceedings Volumes, Volume 15, Issue 4, June 1982, Pages 1149-1154